Hindawi
Journal of Nanomaterials
Volume 2019, Article ID 5961563, 12 pages
https://doi.org/10.1155/2019/5961563

Research Article

Dielectric and Structural Properties of Poly(vinylidene fluoride) (PVDF) and Poly(vinylidene fluoride-trifluoroethylene) (PVDF-TrFE) Filled with Magnesium Oxide Nanofillers

A. N. Arshad,[1] M. H. M. Wahid,[1] M. Rusop,[2] W. H. A. Majid,[3] R. H. Y. Subban,[1] and M. D. Rozana[1]

[1]*Faculty of Applied Sciences, Universiti Teknologi MARA (UiTM), 40450 Shah Alam, Selangor, Malaysia*
[2]*NANO-SciTech Centre (NST), Institute of Science (IOS), Universiti Teknologi MARA (UiTM), 40450 Shah Alam, Selangor, Malaysia*
[3]*Low Dimensional Research Centre, Faculty of Science, Universiti Malaya, 50603 Kuala Lumpur, Malaysia*

Correspondence should be addressed to M. D. Rozana; rozanadahan@gmail.com

Received 27 March 2018; Revised 30 October 2018; Accepted 12 February 2019; Published 21 April 2019

Academic Editor: Ali Khorsand Zak

Copyright © 2019 A. N. Arshad et al. This is an open access article distributed under the Creative Commons Attribution License, which permits unrestricted use, distribution, and reproduction in any medium, provided the original work is properly cited.

This study examines the dielectric properties of filled PVDF film and filled PVDF-TrFE film incorporated with 1, 3, 5, and 7 weight percentages of magnesium oxide (MgO) nanofillers. The metal-insulator-metal (MIM) configuration demonstrates PVDF/MgO with 7 weight percent of MgO which produced high dielectric constant (1 kHz) with low dielectric loss. The ATR-FTIR spectra of PVDF/MgO (7%) indicate wide bonding peaks at 840 cm^{-1} and 880 cm^{-1}, assigned to -CH_2 and -CF_2 groups, respectively. This implies the presence of high content of β-crystals in the PVDF/MgO (7%) film. A shift in the peak was observed in the same film, from 1170 cm^{-1} to 1180 cm^{-1} suggesting possible transformation from γ-crystals to β-crystals. This film showed no apparent defect on its film surface. Thus, it established that PVDF incorporated with 7% MgO can be used to produce nanocomposite thin film for low-frequency electronic devices.

1. Introduction

Polyvinylidene fluoride (PVDF) and its copolymer, polyvinylidene fluoride-trifluoroethylene (PVDF-TrFE), are polymeric materials typically used for electronic applications. PVDF is a semicrystalline polymer, which consists of a repeating unit, -CH_2CF_2 monomer. The dipole moment in PVDF arises from its high electronegativity of fluorine atom and hydrogen atom. The vacuum dipole moment of $\mu_v = 7.0 \times 10^{-30}$ cm or 2.1 Debye was reported for PVDF [1, 2]. Upon crystallization of PVDF, the orientation of dipoles is directly controlled by the molecular conformation and packing of their molecules. Depending on the crystallization conditions of PVDF, different phases of crystal can be formed either as *trans*- (T) or *gauche* (G) linkage of a VDF monomer. There are four major crystal phases in PVDF, identified as α, β, γ, and δ crystals. In the α-phase, the net polarization is zero, due to cancellation of the fluorine atoms [3, 4]. Meanwhile, the δ-phase is a mirror-like of α-phase with orthorhombic lattice, obtained by polarizing α-phase crystals at high electric field (1.25 mV/cm) [5]. The β-phase PVDF has very high dipole moment due to the alignment of all dipole chains in a single direction. This all-*trans* (TTTT) configuration produces high spontaneous polarization in a unit cell, an excellent property for pyro-, piezo-, and ferroelectric film [6, 7]. The final crystalline phase in PVDF is a γ-phase with TTTG-TTTG′ conformation. The γ-phase PVDF is obtained from high-temperature crystallization. It has an orthorhombic structure similar to the β-phase crystal.

Copolymerization of VDF and TrFE induces crystallization of β-phase crystals directly from either melt or solution [8, 9]. The large amount of bulky fluorine atom derived from TrFE monomer creates large hindrance in the molecular structure. It is not able to accommodate the TG+TG-

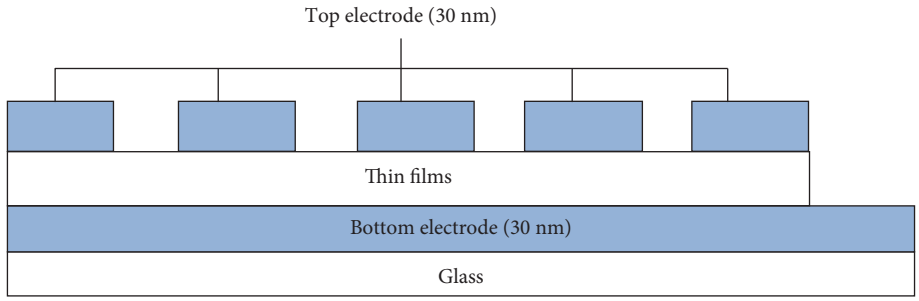

Figure 1: MIM configuration for PVDF and PVDF-TrFE thin films for electrical measurements.

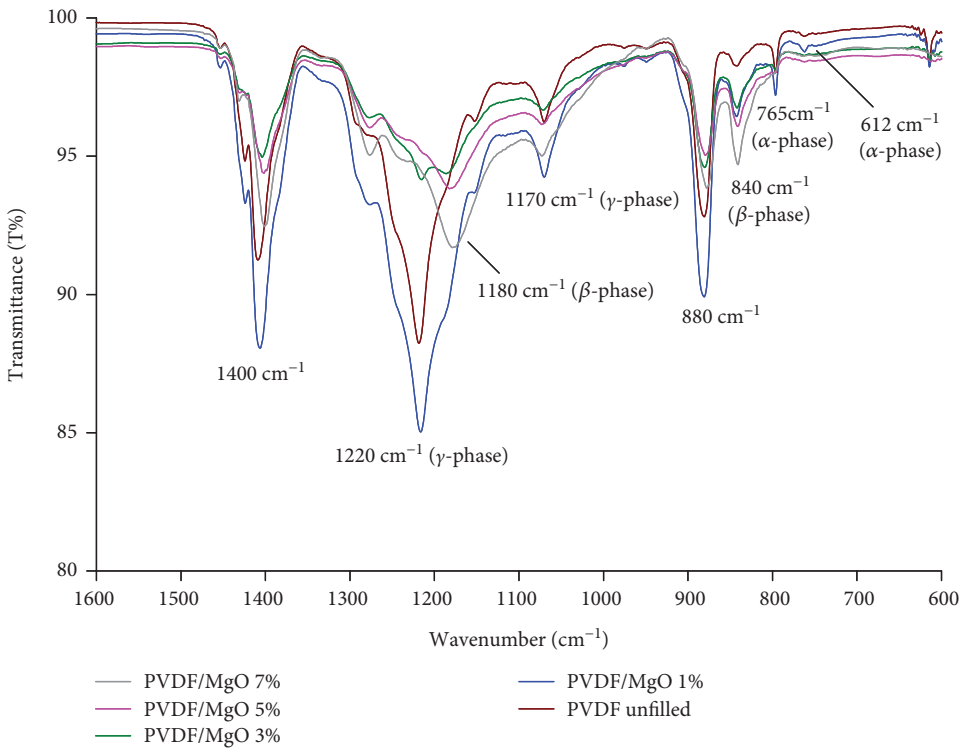

Figure 2: ATR-FTIR transmittance spectra for PVDF unfilled, PVDF/MgO (1%), PVDF/MgO (3%), PVDF/MgO (5%), and PVDF/MgO (7%).

conformation and thus favors all-*trans* conformation. However, the expansion of intermolecular distance due to the presence of TrFE makes the all-*trans* conformation less stable compared to the β-phase in pure PVDF [10, 11].

There are several methods used to enhance the dielectric properties of PVDF, such as mechanical stretching, poling at the electric field, and heat treatment, as well as by incorporation of nanofillers in the PVDF matrix. These treatments are employed individually or combined to obtain specific chain conformation in PVDF, as well as to improve its crystal phases. Conventionally, polymeric materials are typically loaded with inorganic compound to improve its properties, such as physical, mechanical, and functional properties, or simply to reduce the cost of material. Semiconducting fillers such as zinc oxide (ZnO) and titanium dioxide (TiO_2) are common fillers used to enhance the structural and dielectric properties of PVDF. However, it is reported that no modification of crystal phase transition in PVDF is obtained [12–14]. A study made by Tawansi et al. and Saaid et al. [13, 15] discovered that the α- and β-crystal contents of PVDF were greatly increased by inclusion of insulative fillers such as MgO in PVDF. This finding was supported by Paleo and coworkers [16]. They discovered that, with the incorporation of core shell MgO (co-MgO) in solution casting PVDF, the nucleation of γ-polymorph was induced, and β-phase was obtained when the solution is crystallized at room temperature.

According to most findings, the incorporation of inorganic fillers in PVDF induces a crystalline structure due to nucleation sites. This transforms the predominant nonpolar α-phase of PVDF to polar β-phase [16]. However, findings on the dielectric properties of both PVDF homopolymer and PVDF-TrFE copolymer, to a large extent, are not reported. Thus, in this study, MgO inclusion in PVDF and PVDF-TrFE individually which produced composite materials, with the objective to enhance their dielectric properties, was conducted.

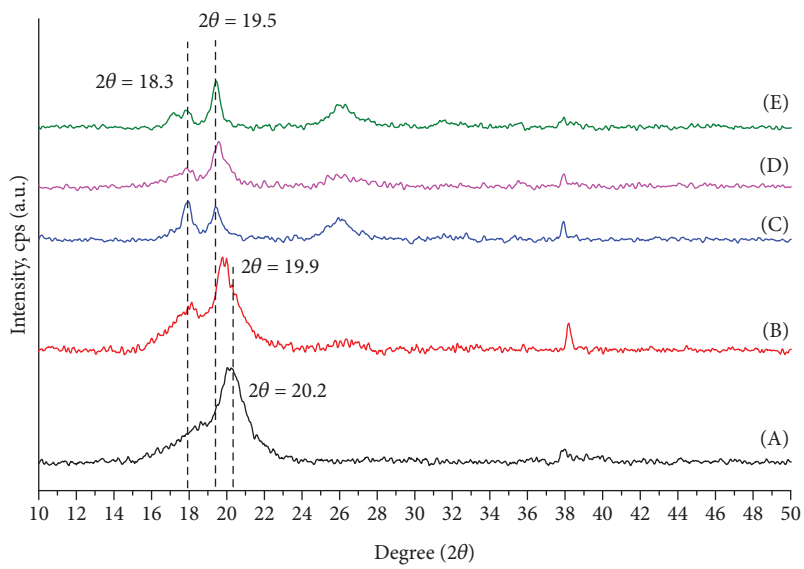

Figure 3: XRD pattern for (a) unfilled PVDF, (b) PVDF/MgO (1%), (c) PVDF/MgO (3%), (d) PVDF/MgO (5%), and (e) PVDF/MgO (7%) thin films.

Table 1: The intensity values of the XRD peaks for PVDF thin film incorporated with 1%, 3%, 5%, and 7% of MgO nanofillers.

Denotations	Count per second (cps)			
	$2\theta = 18.3^\circ$	$2\theta = 19.5^\circ$	$2\theta = 19.9^\circ$	$2\theta = 20.2^\circ$
Unfilled PVDF	—	—	—	700
PVDF/MgO (1%)	325	—	675	—
PVDF/MgO (3%)	275	250		
PVDF/MgO (5%)	150	325	—	—
PVDF/MgO (7%)	125	350	—	—

Miniaturization is a current technology due to the demand for small and lightweight electronic devices. PVDF/MgO and PVDF-TrFE/MgO nanocomposite thin film produced in this study will be a suitable material for minute electronic devices. Importantly, the utilization of this nanocomposite thin film, at low frequency, is favorable for low operational frequency devices operating at low energy.

2. Materials and Methods

2.1. Preparation of Substrates. Glass slides of dimension 2.5 cm × 2.5 cm were used as substrates. Prior to utilization, these glass slides were cleaned with acetone, methanol, and deionised water in a water bath, then sonicated for 10 minutes. For dielectric measurement, aluminium (Al) was evaporated on the cleaned glass substrates, as bottom electrode by using a thermal evaporator (Edwards 306 Turbo, UK). The Al wires were cleaned with acetone to remove any oxide residue and deposited at a slow rate, until the thickness of the evaporated Al reached 30 nm (as indicated by the evaporator built-in thickness gauge meter). The thermal evaporator vacuum pressure was fixed at 2×10^{-5} Mbar and the current at 2 amperes. These Al-coated glass substrates were allowed to cool in the vacuum chamber for 5 minutes before removal. The substrates were stored in a clean glass plastic holder and placed in a desiccator for drying. A mask, 2.5 cm × 2 .5 cm with a square cut out area of 0.09 cm^2, was fabricated to produce a top electrode for the polymeric film. Aluminium (Al) layer, 30 nm thick, was deposited on top of the nanocomposite thin film. The metal-insulator-metal (MIM) configuration was then used for dielectric measurement (Figure 1). Aluminium was used as a dielectric contact due to its ability to resist corrosion and low cost and because it is readily available, compared to gold and platinum electrodes. Most importantly, aluminium has high Coulombic efficiency (~99.7%) [17]. All films were stored in a clean glass plastic holder and kept in desiccators ready for analysis.

2.2. Preparation of PVDF and PVDF-TrFE Thin Films. PVDF powders with a molecular weight of ~534,000 g·mol, obtained from Sigma-Aldrich, and PVDF-TrFE (70 : 30 mol%) powder, obtained from Piezotech, were utilized as purchased. The polymer solutions were prepared by individually dissolving these powders in methyl ethyl ketone (MEK) at a concentration of 30 g/L. They were stirred for 24 hours to ensure complete dissolution. The PVDF and PVDF-TrFE thin films were obtained by spin coating 0.5 mL of these solutions on individual glass substrates at a speed of 1500 rpm for 90 seconds. The thin films were annealed for an hour at 120°C.

2.3. Magnesium Oxide as Filler in a Nanocomposite Thin Film. MgO is proposed in this study due to its chemical inertness and relatively high dielectric properties [18]. It exhibits relatively high dielectric constant value compared to other oxide materials, such as zinc oxide (ZnO) [19]. MgO is also an ideal dielectric material for the fabrication of electronic devices such as capacitor, transistor, and memory devices [16, 20, 21]. A considerable amount of literature has reported deposition and characterization of MgO as a thin layer on substrates [20–24]. Improvement in device characteristics can be achieved for MgO particles within the range of 42 to 84 nm [25].

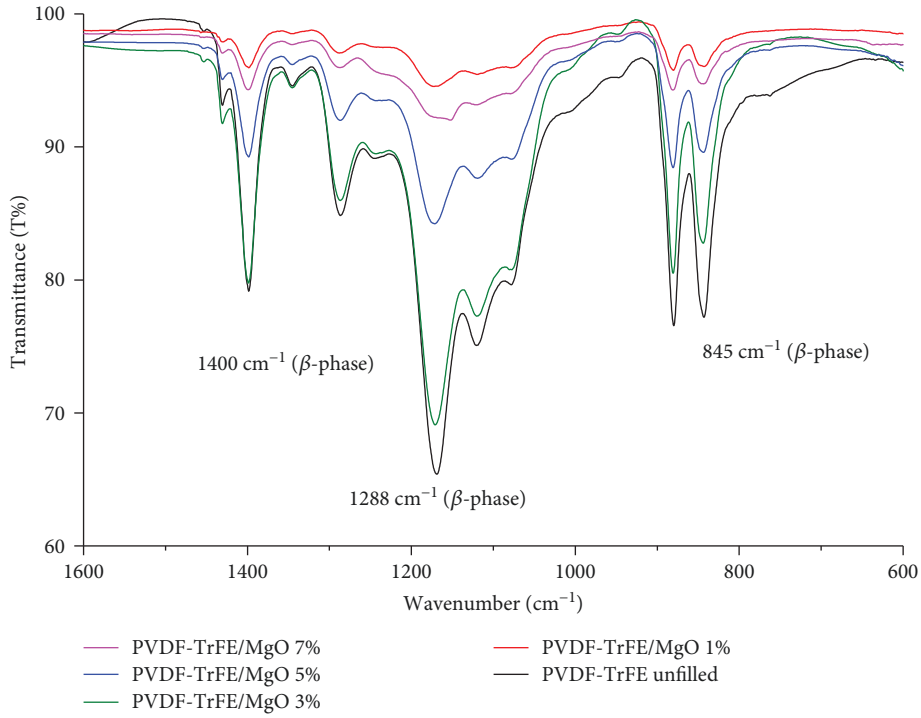

Figure 4: ATR-FTIR spectra for unfilled PVDF-TrFE, PVDF-TrFE/MgO (1%), PVDF-TrFE/MgO (3%), PVDF-TrFE/MgO (5%), and PVDF-TrFE/MgO (7%).

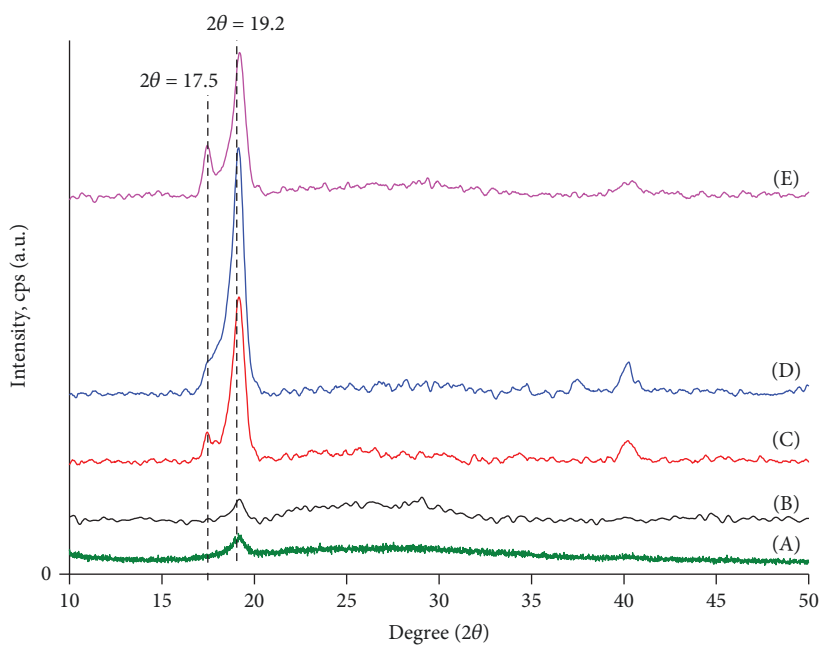

Figure 5: XRD pattern for (a) unfilled PVDF-TrFE, (b) PVDF-TrFE/MgO (1%), (c) PVDF-TrFE/MgO (3%), (d) PVDF-TrFE/MgO (5%), and (e) PVDF-TrFE/MgO (7%).

Dammak and coworkers reported that annealing of MgO nanoparticle at 300°C for 2 hours was essential to remove the moisture and contamination, as well as to allow vaporization of solvent and precursor during processing [24]. This promotes better MgO particle distribution in the polymer matrix. The annealing treatment of MgO powder resulted in improved crystallinity, contributed by the formation of large MgO crystallite, as observed in FESEM [26]. Therefore, in this study, the utilized MgO particles were annealed prior to utilization and processing of PVDF/MgO and PVDF-TrFE/MgO nanocomposite thin films.

2.4. Preparation of PVDF/MgO and PVDF-TrFE/MgO Thin Films. Magnesium oxide (MgO) nanofillers, obtained from

Table 2: The intensity values of the XRD peaks for PVDF-TrFE thin film incorporated with 1%, 3%, 5%, and 7% of MgO nanofiller at 2 $\theta = 17.5^\circ$ and 19.2°.

Denotations	Count per second (cps)	
	$2\theta = 17.5^\circ$	$2\theta = 19.2^\circ$
PVDF-TrFE/1% MgO	9	120
PVDF-TrFE/3% MgO	182	1362
PVDF-TrFE/5% MgO	166	922
PVDF-TrFE/7%MgO	285	806

Sigma-Aldrich with average size of ~100 nm, were pretreated by annealing for 1 hour at 300°C, prior to utilization. MgO nanofillers were dispersed in PVDF and PVDF-TrFE individually at loading percentages of 1, 3, 5, and 7 (wt.%), then stirred for 24 hours. These solutions were spin coated individually on cleaned glass substrates at a speed of 1500 rpm for 90 seconds. The deposited PVDF/MgO and PVDF-TrFE/MgO nanocomposite films were then annealed for 1 hour at 120°C.

2.5. Characterization of Nanocomposite Thin Films. The polymorphism and crystal phases in PVDF/MgO and PVDF-TrFE/MgO nanocomposite films were investigated using attenuated total reflectance Fourier transform infrared (ATR-FTIR) (PerkinElmer). The wavenumbers were set at 1600 cm^{-1} to 650 cm^{-1} with a scan number of 16 and resolution of 4 cm^{-1} per scan. ATR-FTIR spectra were overlaid to observe any changes in the peak intensity. PANanalytical X-ray diffraction (XRD) with nickel filter and Kα of 1.54 A were used to investigate the crystallinity of produced thin films. The scanning angle was set in the range of 5° to 80° with an operating voltage of 45 kV and current of 20 mA. The XRD data were analyzed and replotted using the X'Pert HighScore Plus software. The film's morphology was observed using a field emission scanning electron spectroscope (FE-SEM) (Joel JSM-7600F) at 30K magnification and 5 kV acceleration voltage. Dielectric properties of the nanocomposite thin films at ambient temperature were obtained using an Agilent 4294A high-frequency range impedance analyzer at 100 Hz to 10 MHz frequencies.

3. Result and Discussion

Spin coating result of unfilled PVDF and unfilled PVDF-TrFE was 200 nm and 250 nm in thickness, respectively. The addition of MgO nanofillers showed an increase in the film thickness as determined by a Veeco Dektak surface profiler. PVDF with 1%, 3%, 5%, and 7% MgO produced films with thicknesses of 275 nm, 325 nm, 373 nm, and 458 nm. Meanwhile, PVDF-TrFE/MgO nanocomposites produced a film with thicknesses of 285 nm, 356 nm, 429 nm, and 516 nm for 1%, 3%, 5%, and 7% MgO nanofiller content.

3.1. Effect of MgO Nanofillers on the Crystal Phases of PVDF Nanocomposite Thin Films. Figure 2 illustrates the ATR-FTIR spectra of unfilled PVDF and filled PVDF/MgO nanocomposite at wavenumbers 1600-500 cm^{-1}. The presence of both α- and β-phases denotes typical crystal characteristics of PVDF. PVDF also depicts sharp absorption at 1400 cm^{-1}, indicating an in-plane bending vibration of -CH_2. In addition, the γ-phase at 1170 cm^{-1} and 1220 cm^{-1} was also detected for PVDF thin films. The band of 880 cm^{-1}, attributed to the amorphous phase of PVDF [27]. Absorption band at 840 cm^{-1} was also observed. 840 cm^{-1} is a typical peak for either β- or γ-phase crystals. A sharp and well-resolved band of 840 cm^{-1} observed in this spectrum indicates β-phase crystal of PVDF [28]. PVDF also showed a characteristic absorption band of well-defined α-phases at 612 cm^{-1} and 765 cm^{-1}. The band at 765 cm^{-1} is assigned to the rocking vibration in the PVDF chain, whilst the bending vibration of -CF_2 is observed at 612 cm^{-1}.

Upon addition of 1% MgO, the peak 1400 cm^{-1} showed a narrow absorption band, indicating a strong in-plane bending of -CH_2. Most absorption bands for PVDF/MgO (1%) remained the same. However, as the loading fillers were increased from 3% to 7%, broader absorption band at 1400 cm^{-1} with decreased intensity can be observed. There was also transformation of phases from the γ-phase at 1220 cm^{-1} to the β-phase at 1180 cm^{-1} which indicated wagging vibration of -CH_2. Absorption bands at 765 cm^{-1} and 612 cm^{-1} diminished indicating eradication of α-phases in PVDF/MgO 3%, 5%, and 7%, nonpolar phases of PVDF with zero-net polarization and unfavorable property.

Figure 3 represents the XRD spectra for unfilled PVDF and filled PVDF/MgO nanocomposite thin films with MgO loading percentages of 1%, 3%, 5%, and 7%. From the XRD pattern, unfilled PVDF indicates the presence of β-phase peak at $2\theta = 20.2^\circ$, referring to the sum of diffraction of plane (110). The addition of MgO resulted in emergence $2\theta = 18.3^\circ$ and 19.9° peaks (PVDF/MgO (1%)) representing plane (020) and (110) characteristic of α-phase crystals. Further increase in MgO nanofillers caused a shifting in the peak of 2θ from 19.9° to 19.5° corresponding to β-PVDF with diffraction plane of (200), plus a reduction in α-phase PVDF as seen by peak $2\theta = 18.3$ (Table 1).

3.2. Effect of MgO Nanofillers on the Crystal Phases of PVDF-TrFE Nanocomposite Thin Films. The FTIR spectra for the PVDF-TrFE thin film incorporated with MgO, PVDF-TrFE/MgO (1%), PVDF-TrFE/MgO (3%), PVDF-TrFE/MgO (5%), and PVDF-TrFE/MgO (7%), are presented in Figure 4. Three important bands relate directly to the orientation of the dipoles in PVDF-TrFE. They are 1400 cm^{-1}, assigned to the -CH_2 wagging vibration, and 1288 $cm^{-1}$and 845 cm^{-1} bands, assigned to the -CF_2 symmetric stretching, with dipoles parallel to the *b*-axis. It is observed that similar peaks were seen for both unfilled PVDF-TrFE and PVDF-TrFE/MgO nanocomposite thin films. This signifies that the MgO incorporated into PVDF-TrFE is a physical inclusion, though some slight differences in peak intensity are observed.

This observation denotes the effect of varying MgO nanofillers incorporated into PVDF-TrFE which can affect the orientation of the dipoles. PVDF-TrFE thin film incorporated with 1% MgO showed relatively low intensity in all the absorption peaks. However, for film loaded with 3% MgO nanofillers, significant increase in the intensity was observed

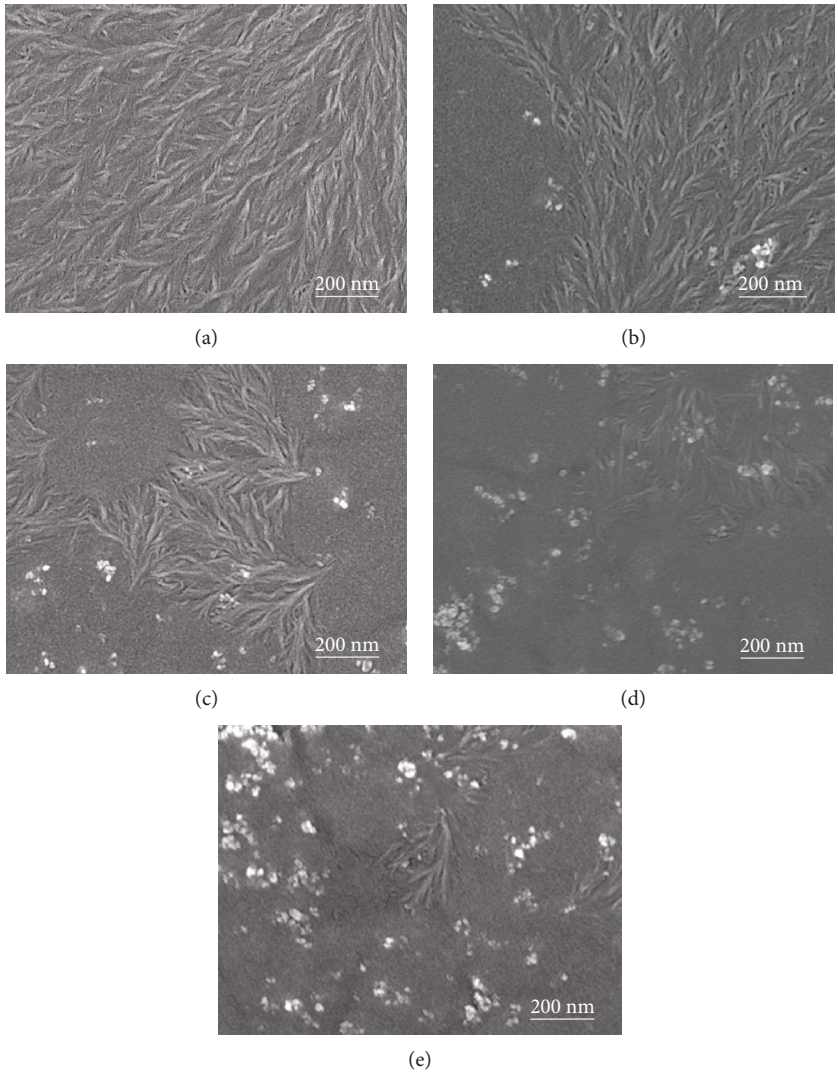

Figure 6: FESEM images of (a) PVDF unfilled, (b) PVDF/MgO (1%), (c) PVDF/MgO (3%), (d) PVDF/MgO (5%), and (e) PVDF/MgO (7%).

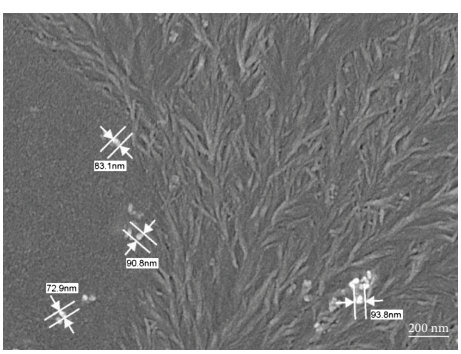

Figure 7: Image of PVDF/MgO (1%) showing the MgO particle size.

for absorption bands of 1400 cm^{-1}, 1288 cm^{-1}, and 845 cm^{-1} for the PVDF-TrFE/MgO (3%) film. These bands are assigned to β-phase crystals, thus, signifying that most of the dipoles in the PVDF-TrFE/MgO (3%) thin film are aligned parallel to the b-axis. However, as soon as the MgO nanofillers percentage loading was further increased to 5%, then 7% intensity of these three peaks decreased quite significantly.

The XRD pattern for PVDF-TrFE thin films incorporated with 1%, 3%, 5%, and 7% MgO nanofillers is shown in Figure 5. The diffraction peaks at $2\theta = 19.2^{\circ}$ denote the presence of β-phase crystals in all nanocomposite thin films. It can be seen that, with the incorporation of MgO nanofillers in annealed PVDF-TrFE thin film, the film showed significant formation of crystal structures in the PVDF-TrFE nanocomposite thin film. This is evident by the well-defined peaks observed at $2\theta = 19.2^{\circ}$ for PVDF-TrFE/MgO (3%) nanocomposite thin film in comparison to 1% MgO loading and unfilled PVDF-TrFE. However, upon increasing the MgO loading percentage to 3% and more, emergence of diffraction peak at $2\theta = 17.5^{\circ}$ relates to the α-phase crystal of PVDF-TrFE [29]. This is not desirable, as the α-phase crystal reduces the dielectric activity of the nanocomposite thin film due to the nonpolar chain crystal conformation of PVDF-TrFE.

The details of XRD peak intensity (cps) are tabulated in Table 2. The thin film incorporated with 1% MgO (PVDF-TrFE/MgO (1%)) showed the lowest $2\theta = 19.2^{\circ}$ peak intensity

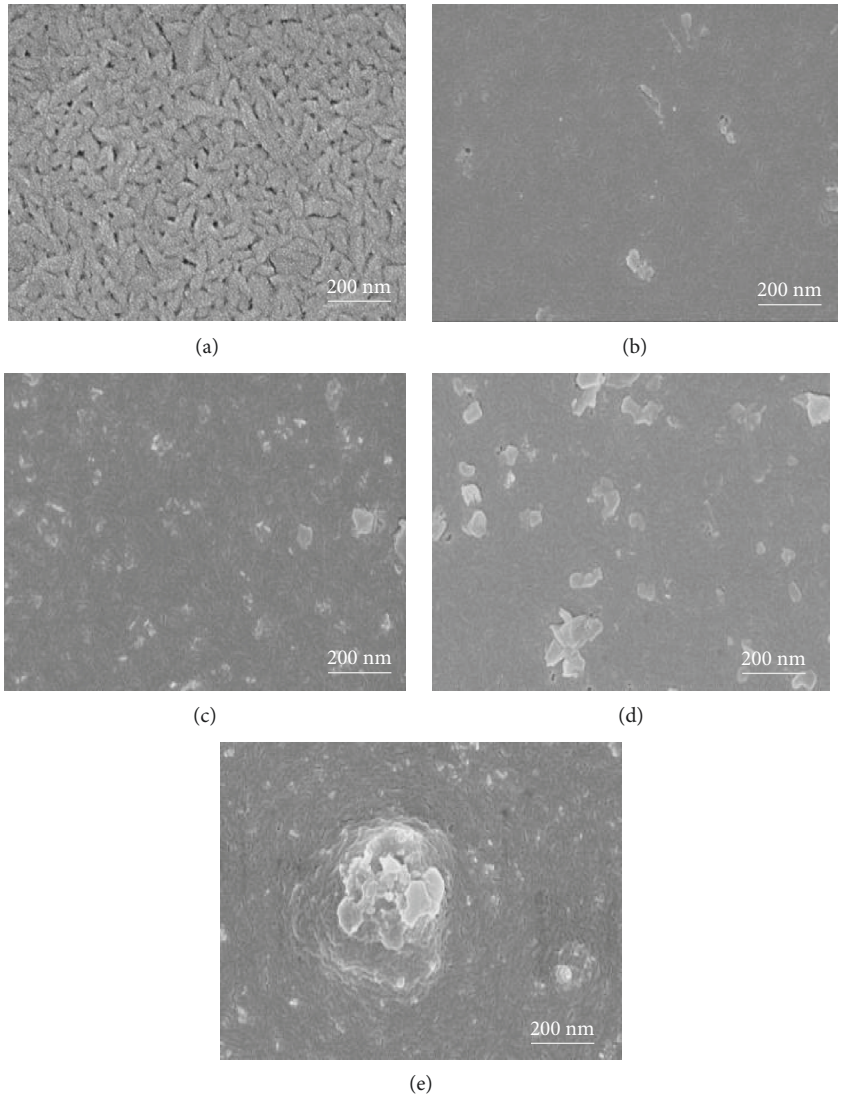

Figure 8: FESEM images of (a) PVDF-TrFE unfilled, (b) PVDF-TrFE/MgO (1%), (c) PVDF-TrFE/MgO (3%), (d) PVDF-TrFE/MgO (5%), and (e) PVDF-TrFE/MgO (7%).

of 120 cps compared to other nanocomposite thin films, with almost absence of peak at $2\theta = 17.5^{\circ}$. This implies that PVDF-TrFE/MgO (1%) thin film retained its β-phase crystal structures. However, the cps value for PVDF-TrFE/MgO (1%) was significantly lower than that for the unfilled PVDF-TrFE thin film. This may be due to small percentages of MgO in the thin film, which was insufficient to improve the crystal structures of PVDF-TrFE/MgO (1%) [30]. With an increase in MgO loading to 3% (PVDF-TrFE/MgO (3%)), the peak of $2\theta = 19.2^{\circ}$ significantly increased by onefold (1362 cps) due to induced molecular chain packing which formed a highly ordered crystalline structure of PVDF-TrFE.

However, the film incorporated with 5% MgO (PVDF-TrFE/MgO (5%)) showed 32% reduction of $2\theta = 19.2^{\circ}$ peak. Similarly, the 7% MgO nanocomposite thin film showed decrement of $2\theta = 19.2^{\circ}$ peak intensity by 40% in comparison to the PVDF-TrFE/MgO (3%) thin film. Moreover, these MgO nanofillers may act as secondary nucleating sites in promoting the formation and growth of the crystalline phase of PVDF-TrFE [31]. However, there is a limitation to the percentage of MgO nanofillers incorporated in PVDF-TrFE nanocomposite films. This is shown by a significant diffraction peak at 17.5° for the film loaded with 7% MgO, indicating the presence of α-phase crystal structure in the film. At this point, the high MgO loading percentage actually disrupts the PVDF-TrFE chain alignment and reverts the β-phase to α-phase crystal structure [29, 32]. Thus, this suggests that 3% MgO is the optimized loading percentage for β-enhanced PVDF-TrFE/MgO nanocomposite thin film. This is evident from the highest diffraction peak of $2\theta = 19.2^{\circ}$, as well as the low diffraction peak of $2\theta = 17.5^{\circ}$.

3.3. Effect of MgO Nanofillers on the Morphology of PVDF Nanocomposite Thin Films. Figures 6(a)–6(e) illustrate the FESEM images of PVDF unfilled, PVDF/MgO (1%), PVDF/MgO (3%), PVDF/MgO (5%), and PVDF/MgO (7%), respectively. As the filler loading increases, the size of the tree-like PVDF spherulite decreases. The growth of the

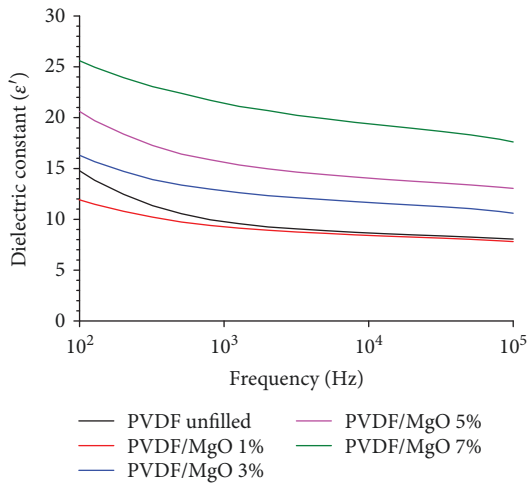

Figure 9: Dielectric constant versus frequency of PVDF unfilled, PVDF/MgO (1%), PVDF/MgO (3%), PVDF/MgO (5%), and PVDF/MgO (7%).

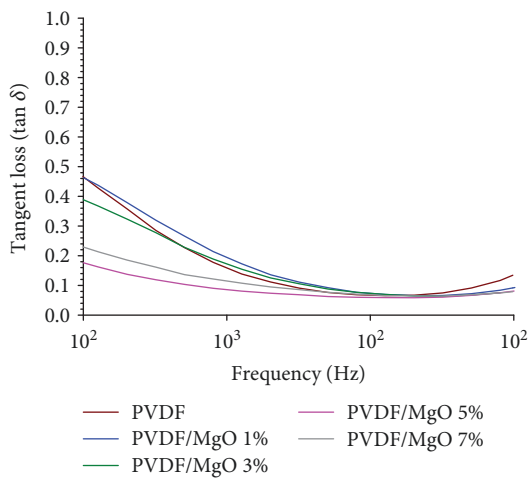

Figure 10: Tangent loss versus frequency of PVDF unfilled, PVDF/MgO (1%), PVDF/MgO (3%), PVDF/MgO (5%), and PVDF/MgO (7%).

spherulites was hindered, resulting in the formation of short-sized spherulites. This observation is more prominent for PVDF/MgO (5%) and PVDF/MgO (7%) films, which suggests that excess of MgO nanofillers will produce secondary nucleating sites promoting growth of smaller spherulites, which assists in dispersing MgO nanofillers in the PVDF matrix. This is shown by white specks of MgO in the PVDF/MgO (1%) and PVDF/MgO (3%) films. However, clusters of MgO were apparent in PVDF/MgO (5%) and PVDF/MgO (7%) films. The size of the MgO particles is in the range of 72 nm to 98 nm (Figure 7).

3.4. Effect of MgO Nanofillers on the Morphology of PVDF-TrFE Nanocomposite Thin Films. As for PVDF-TrFE film incorporated with MgO nanofillers, the 1% MgO nanofiller film showed dominant elongated fibrillar-like crystallites of PVDF-TrFE (Figure 8). At 3% MgO loading, the distribution of the MgO was obvious throughout the PVDF-TrFE/MgO (3%) nanocomposite thin film. This is shown as white specks in the film alongside defined and elongated shape PVDF-TrFE crystallites. Again, these MgO nanofillers created favorable nucleating sites for crystallite to grow in the PVDF-TrFE/MgO (3%) nanocomposite thin film. The films show homogenous dispersion of MgO on PVDF-TrFE films.

Upon increasing the MgO loading to 5%, agglomerates of MgO fillers were fairly visible for the PVDF-TrFE/MgO (5%) thin film (Figure 8(d)). With further increase of MgO loading to 7%, large clusters of MgO were observed in the PVDF-TrFE/MgO (7%) film (Figure 8(e)). Meanwhile, rippled-like PVDF-TrFE crystallites replaced the elongated PVDF-TrFE crystallites (as seen in the unfilled PVDF-TrFE film). This finding is consistent with the FTIR analysis, which showed low intensity of FTIR peaks, suggesting loss in dipole alignment in the PVDF-TrFE/MgO (7%) film.

3.5. Effects of MgO Nanofillers on the Dielectric Properties of PVDF Nanocomposite Thin Films. The dielectric constant versus the frequency curve shown in Figure 9 indicates a similar trend for both unfilled PVDF and PVDF/MgO nanocomposite films: decreasing of dielectric constant with increasing frequency. However, the dielectric constant was observed to plateau between 1 kHz and 10 kHz frequency. But at a very low frequency of 100 Hz, the dielectric constant value was relatively high, due to polarization orientation of the PVDF chain structure caused by permanent dipole moment. MgO dielectric constant is 7.4 at 1 kHz as reported by Habibah et al. [33]. The dielectric constant value obtained for unfilled PVDF was 10 at 1 kHz, higher than that reported by other studies [34, 35]. However, slight decrement in the dielectric constant value at the same frequency was observed with inclusion of 1% MgO in PVDF.

With the further increasing of MgO nanofiller loading from 3% to 5% in PVDF, an increase in dielectric constant for PVDF/MgO nanocomposite at 1 kHz was observed in comparison to unfilled PVDF-TrFE, that is, 13 for PVDF/MgO (3%) and 15 for PVDF/MgO (5%). Interestingly, PVDF loaded with 7% MgO showed the highest dielectric constant value (22) amongst these filled PVDF films. This is due to polarizability of PVDF upon the application of the electric field caused by an increase in polarized charges due to the dipolar contribution of MgO nanofiller.

The tangent loss (tan δ) of PVDF unfilled and PVDF/MgO nanocomposite is shown in Figure 10. As reported by a previous study, the tangent loss for MgO is 0.02 [33]. From Figure 10, tan δ decreased as the frequency is increased. Tan δ for the PVDF unfilled and PVDF/MgO nanocomposite was below 1.0, indicating that energy dissipation for both the PVDF unfilled and PVDF/MgO nanocomposite is relatively low.

As observed from Figure 10, tan δ at a frequency of 100 to 1 kHz for the PVDF unfilled was slightly high compared to that for the PVDF/MgO nanocomposite. Tan δ was observed to decrease as the loading of MgO is increased. PVDF/MgO (7%) recorded the lowest tan δ at a frequency of 100 Hz that is 0.4. The tan δ for PVDF/MgO (7%) continues to decrease with the increase

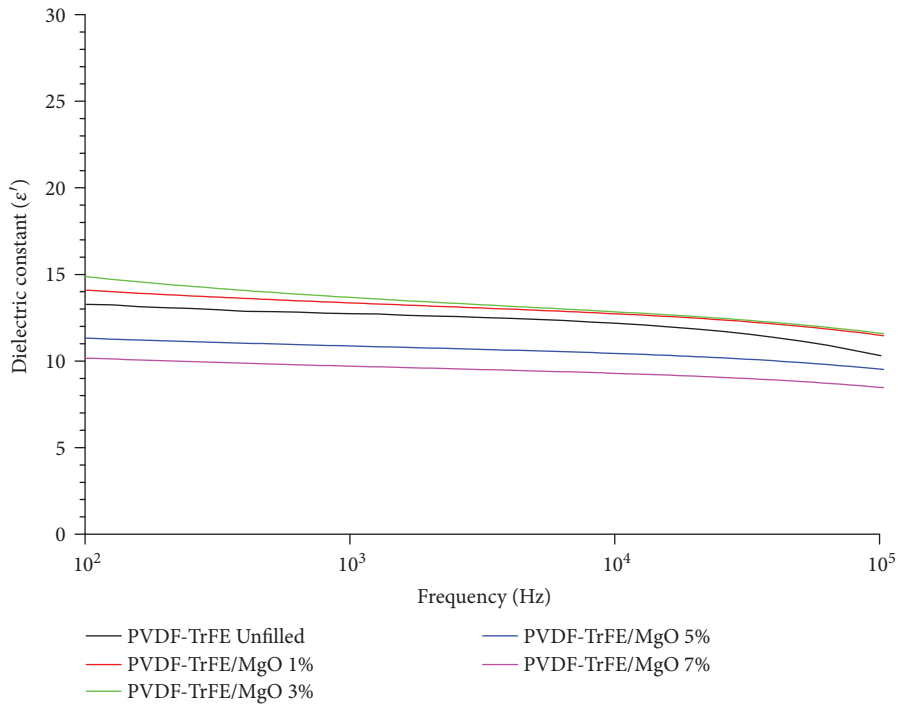

Figure 11: Dielectric constant versus frequency of PVDF-TrFE unfilled, PVDF-TRFE/MgO (1%), PVDF-TRFE/MgO (3%), PVDF-TRFE/MgO (5%), and PVDF-TRFE/MgO (7%).

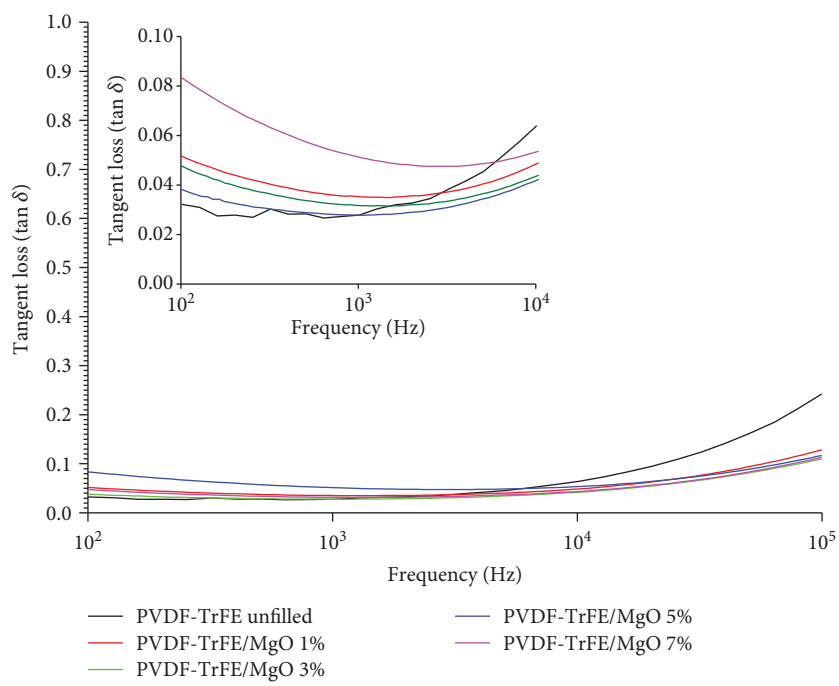

Figure 12: Dielectric constant versus frequency and tangent loss (inset) of PVDF-TrFE unfilled, PVDF-TRFE/MgO (1%), PVDF-TRFE/MgO (3%), PVDF-TRFE/MgO (5%), and PVDF-TRFE/MgO (7%).

in frequency. When alternating current is applied, the dipoles responsible for the polarization are no longer able to follow the oscillation of the electric field at these frequencies. At high frequency, the field reversal and dipole reorientation are out of phase and caused an increase in the dielectric relaxation.

3.6. Effects of MgO Nanofillers on the Dielectric Properties of PVDF-TrFE Nanocomposite Thin Films. The relationship between dielectric constant frequency and tangent loss frequency for the unfilled PVDF-TrFE and filled PVDF-TrFE/MgO is presented in Figures 11 and 12, respectively. The trend shows an increase in the dielectric constant for

Table 3: Comparison study on the dielectric constant value at 1 kHz for PVDF/MgO and PVDF-TrFE/MgO.

Author	Findings	Ref.
Mahdi et al.	Film prepared by solution casting with thickness of 25 μm. Dielectric constant was obtained for unfilled PVDF-TrFE 7.2 at 1 kHz, with tangent loss of 0.1 at similar frequency.	[37]
Singh et al.	PVDF-TrFE/MgO prepared by solution casting with 20 μm thick film. However, no dielectric constant value was recorded.	[38]
Chen et al.	Addition of MgO into PVDF with varying loading percentage between 1 and 4%. The dielectric constant value decreased with increase in MgO loading. Dielectric constant recorded at a frequency of 1 kHz was 7.5.	[39]

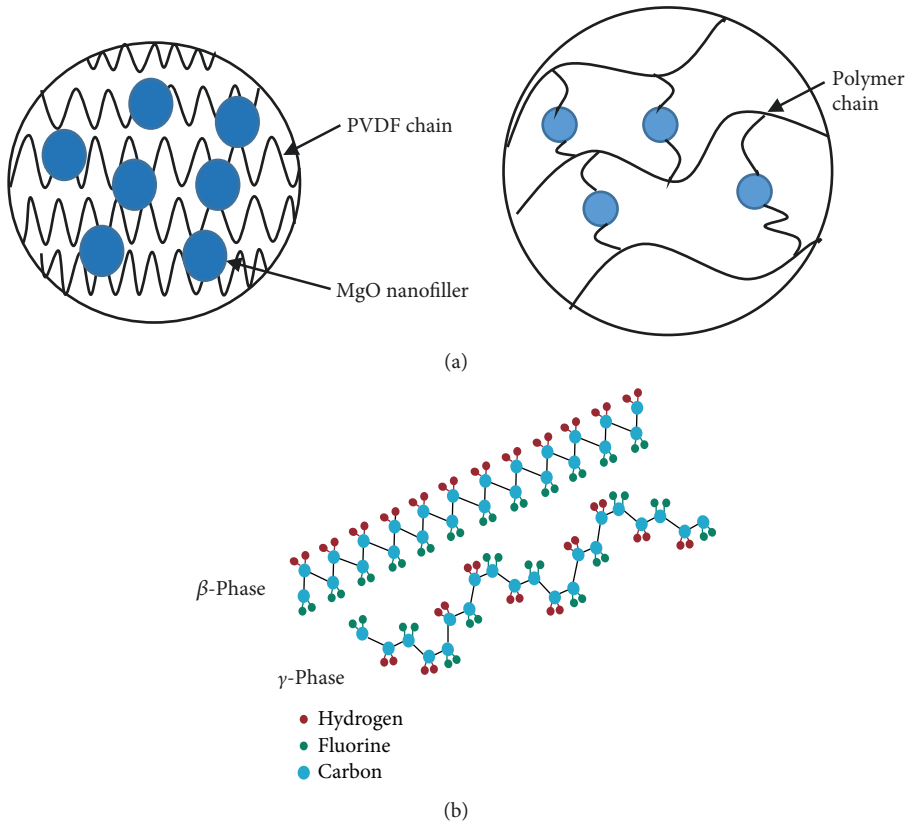

Figure 13: Schematic representation of (a) PVDF/MgO nanocomposites showing the networking of MgO nanofillers in PVDF and (b) chemical configuration of γ- and β-phase crystals of PVDF.

filled PVDF-TrFE/MgO films up to 3% MgO loading. This may be due to the interfacial polarization between polymer and nanofillers. The large-scale distortion of polarization occurs due to the near existence of the dielectric property of MgO and highly polarized PVDF-TrFE caused by application of an electric field [33, 36]. The average charge increases with an increase in the polar dipoles in PVDF-TrFE as well as the dipolar contribution of MgO nanofillers [9, 34].

Initially, the dielectric constant for the PVDF-TRFE/MgO (1%) film at 1 kHz frequency was 13.4. At the same frequency, the dielectric constant for the PVDF-TrFE/MgO (3%) film increased to 13.7 due to enhancement of β-crystal in the film and increased in dipolar polarization. As MgO loading was increased to 5% and 7%, reduction in dielectric constant value was observed, at similar frequency: 10.9 and 9.7, respectively. This significant drop in the dielectric constant value corresponds to less polarized dipoles in the nanocomposite thin films due to low β-crystal structure, evident from the FTIR spectra. The decrease in dielectric constant value was fully supported by the morphology of the PVDF-TrFE/MgO (5%) and PVDF-TrFE/MgO (7%) film. The FESEM image showed rippled-like crystallite structures rather than elongated PVDF-TrFE crystallites as observed in the PVDF-TRFE/MgO (1%) film. There was also cluster and agglomerations of MgO in the film.

The dielectric constant of PVDF-TrFE recorded for this study is slightly higher compared to that for a study conducted by Mahdi et al., which is 7.2 at 1 kHz for the unfilled PVDF-TrFE [37]. The dielectric constant recorded for this study was 13 at similar frequency. Singh et al. also conducted a study on PVDF-TrFE with the addition of MgO nanofillers (20 μm thick). However, no dielectric constant value was recorded [38]. Chen et al. conducted a study with addition of MgO with varying loading percentage into PVDF and

solution casted to form a 25 μm thick film. The investigation showed a reduction in the dielectric constant at similar frequency (1 kHz). Nevertheless, the tangent loss value was also decreased [39]. The comparison study is tabulated in Table 3.

3.7. Proposed Interaction Mechanism of PVDF and MgO Particles. The proximity and interaction of the PVDF chain and nanosized MgO particles (<100 nm) are shown schematically in Figure 13(a). During annealing of the nanocomposite film, segmental PVDF chain motion caused displacement and distribution of MgO nanoparticles due to the thermal heating. This process continues and promotes the interaction between PVDF chain dipole and MgO, which latched MgO particles onto the PVDF polymer chain. The nanosized MgO particles are receptive to this segmental PVDF chain motion and caused secondary nucleation. This leads to the enhancement of the crystallization of the PVDF/MgO structure. This is supported by the FTIR result as discussed earlier that caused the shifting of the γ-phase to β-phase for the PVDF/MgO 7% film. The transformation of the PVDF crystal phase from γ-phase to β-phase is due to the conversion of its crystal configuration. The γ-phase PVDF is conformed to TTTG configuration, whilst the β-phase PVDF is conformed to all-*trans* configuration, TTTT (Figure 13(b)). As most of the dipoles are pointing in the same direction, the TTTT configuration has the highest net dipole moments compared to the γ-phase and hence desirable for a dielectric film [6, 7]. Thus, the study suggests that if MgO is utilized in its optimized amount, it can act as a secondary nucleation site and induces assembly of TTTT conformation of PVDF crystals.

4. Conclusion

As a conclusion, the addition of MgO nanofillers showed better compatibility with homopolymer PVDF compared to copolymer PVDF-TrFE, as evidenced by FTIR analyses and dielectric measurements. PVDF-TrFE/MgO with 3% loading showed an increase in the dielectric constant value of 13.7 at 1 kHz compared to the unfilled PVDF-TrFE (dielectric constant value = 10). However, in the PVDF/MgO with 7% MgO loading, significant enhancement in the dielectric constant value of 22 at 1 kHz was observed. The optimized nanocomposite film also indicates shifting of PVDF crystal phases from γ-crystal to β-crystals, contributing to the increase in the dielectric constant value. PVDF/MgO (7%) showed no apparent defect as observed by FESEM images. Thus, it can be suggested that PVDF/MgO (7%) is capable to be utilized for a low-frequency capacitor.

Data Availability

The data used to support the findings of this study are available from the corresponding author upon request.

Conflicts of Interest

The authors declare that they have no conflicts of interest.

Acknowledgments

The authors would like to acknowledge the Faculty of Applied Sciences (FSG), Microwave Technology Institute (MTI), Faculty of Electrical Engineering, and NANO-SciTech Centre (NST), UiTM, Shah Alam, for their support. This research was fully funded by BESTARI Grant (600-IRMI/DANA 5/3 BESTARI (063/2017)) from Universiti Teknologi MARA (UiTM), Selangor, Shah Alam, Malaysia.

References

[1] T. Furukawa, "Ferroelectric properties of vinylidene fluoride copolymers," *Phase Transitions*, vol. 18, no. 3-4, pp. 143–211, 1989.

[2] V. S. Bystrov, "Molecular modeling and molecular dynamics simulation of the polarization switching phenomena in the ferroelectric polymers PVDF at the nanoscale," *Physica B: Condensed Matter*, vol. 432, pp. 21–25, 2014.

[3] A. Aliane, M. Benwadih, B. Bouthinon, R. Coppard, F. Domingues-Dos Santos, and A. Daami, "Impact of crystallization on ferro-, piezo- and pyro-electric characteristics in thin film P(VDF–TrFE)," *Organic Electronics*, vol. 25, pp. 92–98, 2015.

[4] J.-H. Bae and S.-H. Chang, "Characterization of an electroactive polymer (PVDF-TrFE) film-type sensor for health monitoring of composite structures," *Composite Structures*, vol. 131, pp. 1090–1098, 2015.

[5] N. An, H. Liu, Y. Ding, M. Zhang, and Y. Tang, "Preparation and electroactive properties of a PVDF/nano-TiO_2 composite film," *Applied Surface Science*, vol. 257, no. 9, pp. 3831–3835, 2011.

[6] W. C. Gan, W. H. A. Majid, and T. Furukawa, "Ferroelectric polarization, pyroelectric activity and dielectric relaxation in Form IV poly(vinylidene fluoride)," *Polymer*, vol. 82, pp. 156–165, 2016.

[7] K. Asai, M. Okamoto, and K. Tashiro, "Real-time investigation of crystallization in poly(vinylidene fluoride)-based nanocomposites probed by infrared spectroscopy," *Polymer*, vol. 49, no. 24, pp. 5186–5190, 2008.

[8] J. B. Lando and W. W. Doll, "The polymorphism of poly(vinylidene fluoride). I. The effect of head-to-head structure," *Journal of Macromolecular Science, Part B*, vol. 2, no. 2, pp. 205–218, 1968.

[9] N. Shingne, M. Geuss, B. Hartmann-Azanza, M. Steinhart, and T. Thurn-Albrecht, "Formation, morphology and internal structure of one-dimensional nanostructures of the ferroelectric polymer P(VDF-TrFE)," *Polymer*, vol. 54, no. 11, pp. 2737–2744, 2013.

[10] F. J. B. Calleja, A. G. Arche, T. A. Ezquerra et al., "Structure and properties of ferroelectric copolymers of poly(vinylidene fluoride)„" in *Structure in Polymers with Special Properties*, H. G. Zachmann, Ed., pp. 1–48, Springer, 1993.

[11] T. Furukawa, Y. Takahashi, and T. Nakajima, "Recent advances in ferroelectric polymer thin films for memory applications," *Current Applied Physics*, vol. 10, no. 1, pp. e62–e67, 2010.

[12] M. H. Mamat, M. I. Che Khalin, N. N. H. Nik Mohammad et al., "Effects of annealing environments on the solution-grown, aligned aluminium-doped zinc oxide nanorod-array-

based ultraviolet photoconductive sensor," *Journal of Nanomaterials*, vol. 2012, Article ID 189279, 15 pages, 2012.

[13] F. Saaid, I. Rodi, and T. Winie, "Effect of temperature on the transport property of PVdF-HFP-MPII-PC/DME gel polymer electrolytes," in *AIP Conference Proceedings 2017*, Shah Alam, Malaysia, 2017.

[14] F.-C. Chiu, "Comparisons of phase morphology and physical properties of PVDF nanocomposites filled with organoclay and/or multi-walled carbon nanotubes," *Materials Chemistry and Physics*, vol. 143, no. 2, pp. 681–692, 2014.

[15] A. Tawansi, A. H. Oraby, E. M. Abdelrazek, and M. Abdelaziz, "Structural and electrical properties of MgCl2-filled PVDF films," *Polymer Testing*, vol. 18, no. 8, pp. 569–579, 1999.

[16] A. J. Paleo, C. Martínez-Boubeta, L. Balcells, C. M. Costa, V. Sencadas, and S. Lanceros-Mendez, "Thermal, dielectrical and mechanical response of α and β-poly(vinilydene fluoride)/Co-MgO nanocomposites," *Nanoscale Research Letters*, vol. 6, no. 1, p. 257, 2011.

[17] M. Angell, C. J. Pan, Y. Rong et al., "High Coulombic efficiency aluminum-ion battery using an AlCl3-urea ionic liquid analog electrolyte," *Proceedings of the National Academy of Sciences of the United States of America*, vol. 114, no. 5, pp. 834–839, 2017.

[18] L. Yan, C. M. Lopez, R. P. Shrestha, E. A. Irene, A. A. Suvorova, and M. Saunders, "Magnesium oxide as a candidate high-κ gate dielectric," *Applied Physics Letters*, vol. 88, no. 14, article 142901, 2006.

[19] P. I. Devi and K. Ramachandran, "Dielectric studies on hybridised PVDF–ZnO nanocomposites," *Journal of Experimental Nanoscience*, vol. 6, no. 3, pp. 281–293, 2011.

[20] A. Kumar, S. Thota, S. Varma, and J. Kumar, "Sol-gel synthesis of highly luminescent magnesium oxide nanocrystallites," *Journal of Luminescence*, vol. 131, no. 4, pp. 640–648, 2011.

[21] A. Posadas, F. J. Walker, C. H. Ahn, T. L. Goodrich, Z. Cai, and K. S. Ziemer, "Epitaxial MgO as an alternative gate dielectric for SiC transistor applications," *Applied Physics Letters*, vol. 92, no. 23, article 233511, 2008.

[22] F. Mohandes, F. Davar, and M. Salavati-Niasari, "Magnesium oxide nanocrystals via thermal decomposition of magnesium oxalate," *Journal of Physics and Chemistry of Solids*, vol. 71, no. 12, pp. 1623–1628, 2010.

[23] P. Casey, E. O'Connor, R. Long et al., "Growth, ambient stability and electrical characterisation of MgO thin films on silicon surfaces," *Microelectronic Engineering*, vol. 86, no. 7-9, pp. 1711–1714, 2009.

[24] N. Dammak, F. Trigui, T. Temga, A. Kallel, Z. Fakhfakh, and D. Treheux, "Study of charging phenomena in MgO single crystal: effect of polishing, annealing temperature and crystallographic orientation," *Journal of the European Ceramic Society*, vol. 22, no. 7, pp. 1149–1154, 2002.

[25] Z. Habibah, A. N. Arshad, M. H. Wahid et al., "Properties of ZnO/MgO multilayer films as insulating layer prepared by sol-gel method," in *2012 10th IEEE International Conference on Semiconductor Electronics (ICSE)*, Kuala Lumpur, Malaysia, 2012.

[26] H. S. Jung, J. K. Lee, J. Y. Kim, and K. S. Hong, "Crystallization behaviors of nanosized MgO particles from magnesium alkoxides," *Journal of Colloid and Interface Science*, vol. 259, no. 1, pp. 127–132, 2003.

[27] N. Jia, Q. He, J. Sun, G. Xia, and R. Song, "Crystallization behavior and electroactive properties of PVDF, P(VDF-TrFE) and their blend films," *Polymer Testing*, vol. 57, pp. 302–306, 2017.

[28] J. Arranz-Andrés, N. Pulido-González, C. Fonseca, E. Pérez, and M. L. Cerrada, "Lightweight nanocomposites based on poly(vinylidene fluoride) and Al nanoparticles: structural, thermal and mechanical characterization and EMI shielding capability," *Materials Chemistry and Physics*, vol. 142, no. 2-3, pp. 469–478, 2013.

[29] A. Lund, C. Gustafsson, H. Bertilsson, and R. W. Rychwalski, "Enhancement of β-phase crystals formation with the use of nanofillers in PVDF films and fibres," *Composites Science and Technology*, vol. 71, no. 2, pp. 222–229, 2011.

[30] V. S. Nguyen, D. Rouxel, B. Vincent et al., "Influence of cluster size and surface functionalization of ZnO nanoparticles on the morphology, thermomechanical and piezoelectric properties of P(VDF-TrFE) nanocomposite films," *Applied Surface Science*, vol. 279, pp. 204–211, 2013.

[31] M. L. Di Lorenzo, "Spherulite growth rates in binary polymer blends," *Progress in Polymer Science*, vol. 28, no. 4, pp. 663–689, 2003.

[32] W. C. Gan and W. H. A. Majid, "Effect of TiO_2 on enhanced pyroelectric activity of PVDF composite," *Smart Materials and Structures*, vol. 23, no. 4, article 045026, 2014.

[33] Z. Habibah, K. A. Yusof, L. N. Ismail, R. A. Bakar, and M. Rusop, "Sol-gel derived nano-magnesium oxide: influence of drying temperature to the dielectric layer properties," *IOP Conference Series: Materials Science and Engineering*, vol. 46, article 012006, 2013.

[34] H. J. Chen, S. Han, C. Liu et al., "Investigation of PVDF-TrFE composite with nanofillers for sensitivity improvement," *Sensors and Actuators A: Physical*, vol. 245, pp. 135–139, 2016.

[35] M. Ataur Rahman and G. S. Chung, "Synthesis of PVDF-graphene nanocomposites and their properties," *Journal of Alloys and Compounds*, vol. 581, pp. 724–730, 2013.

[36] A. R. Bueno, R. F. M. Oman, P. M. Jardim, N. A. Rey, and R. R. de Avillez, "Kinetics of nanocrystalline MgO growth by the sol–gel combustion method," *Microporous and Mesoporous Materials*, vol. 185, pp. 86–91, 2014.

[37] R. I. Mahdi, W. C. Gan, and W. H. A. Majid, "Hot plate annealing at a low temperature of a thin ferroelectric P(VDF-TrFE) film with an improved crystalline structure for sensors and actuators," *Sensors*, vol. 14, no. 10, pp. 19115–19127, 2014.

[38] D. Singh, A. Choudhary, and A. Garg, "Flexible and robust piezoelectric polymer nanocomposites based energy harvesters," *ACS Applied Materials & Interfaces*, vol. 10, no. 3, pp. 2793–2800, 2018.

[39] S.-S. Chen, J. Hu, L. Gao et al., "Enhanced breakdown strength and energy density in PVDF nanocomposites with functionalized MgO nanoparticles," *RSC Advances*, vol. 6, no. 40, pp. 33599–33605, 2016.

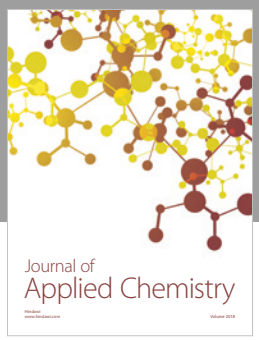

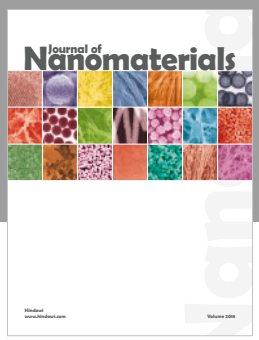

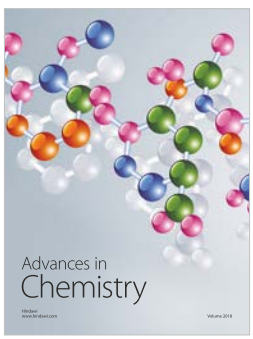

Hindawi

Submit your manuscripts at
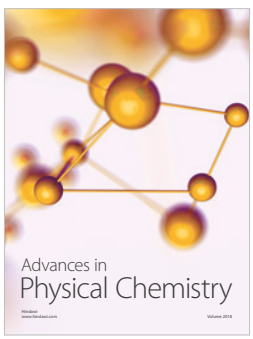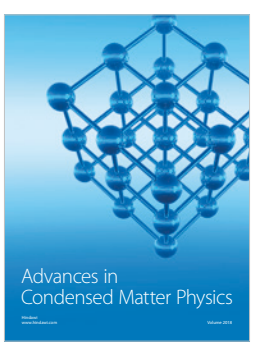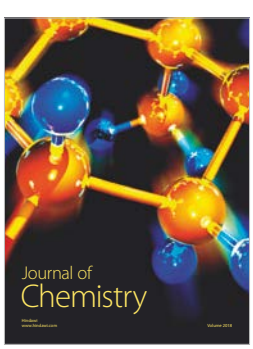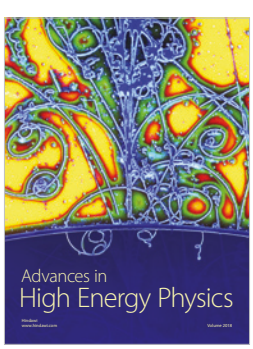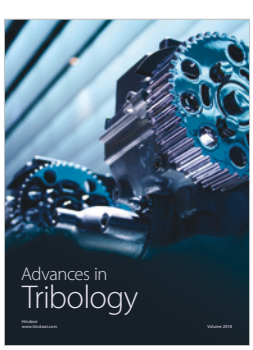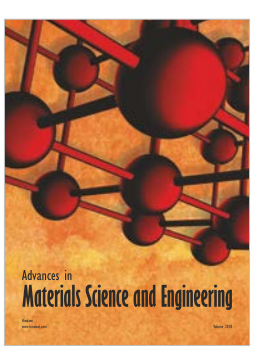
www.hindawi.com